Preprints of the 12th IFAC Symposium on Computer Applications in Biotechnology
The International Federation of Automatic Control
16-18, 2013, December. Mumbai, India

Estimation of Chlamydomonas reinhardtii Growth in a Torus Photobioreactor

Sihem Tebbani*, Mariana Titica, Sergiu Caraman***, Lionel Boillereaux****

**SUPELEC, Systems Sciences (E3S), Control Department,*
F 91192 Gif sur Yvette cedex, France (e-mail: sihem.tebbani@supelec.fr)
*** L'UNAM Université, Université de Nantes, ONIRIS, CNRS, GEPEA, UMR-CNRS 6144University Bd., CRTT-BP 406, 44600, Saint-Nazaire, France*
(e-mail: mariana.titica@univ-nantes.fr, lionel.boillereaux@oniris-nantes.fr)
**** University of Galati, Domneascã Street, no. 47, 800008, Galati, Romania*
(e-mail: sergiu.caraman@ugal.ro)

Abstract: Microalgae culture is used in various biotechnological applications. Optimisation of the system productivity needs reliable sensors. However, physical sensors for biomass and dissolved dioxide carbon concentrations are expensive and not accurate, especially for online measurements. In this context, robust and efficient software sensors have to be developed. In this paper, an Unscented Kalman filter (UKF) methodology is proposed to estimate components concentrations in a photobioreactor. The microalgae *Chlamydomonas reinhardtii* is used as model organism. The aim of this paper is to develop an online software estimator that reconstructs the biomass, carbon dioxide and oxygen concentrations in the liquid phase, from online measurements of components molar fraction in the output gas provided by a mass spectrometer. The proposed estimator is validated through experimental data collected on a lab-scale photobioreactor.

***Keywords**:* Unscented Kalman Filter, microalgae, photobioreactor

1. INTRODUCTION

Microalgae have a great capacity of consumption of carbon dioxide, converting it into biomass and other secondary metabolites such as intracellular polysaccharides, proteins, pigments etc. Large-scale cultures also find applications in energy production (e.g. photobiological hydrogen, biofuel, methane) and environmental remediation (e.g. wastewater treatment, carbon dioxide fixation and greenhouse gas emissions reduction). Microalgae also can absorb heavy metals and sequester or degrade many different classes of toxic compounds.

These applications of cultures of microalgae are developed under optimal conditions, generally in closed systems (photobioreactors). In order to achieve optimal performances, these photosynthetic growth processes must be accurately monitored and controlled. A fundamental step for the implementation of an effective control strategy is to choose a reliable model that can effectively describe the biochemical dynamics of microalgae. Developed mathematical models highlight the influence of light intensity and/or carbon source on biomass growth.

However, due to model and kinetic parameters uncertainty, and for control purposes, online estimators have to be developed, to overcome the lack of physical sensors (not reliable and expensive), especially for biomass concentration.

Thus, designing a robust state observer represents a real challenge in bioprocesses. Several studies have tackled biomass estimation for bioprocesses. The main approaches are based on asymptotic estimator (Bastin and Dochain, 1990), extended Kalman filter (Su *et al.,* 2003) and more recently interval observers (Rapaport *et al.* 2005; Goffaux *et al.*, 2009).

In the case of photobioreactors, the widely used estimator is the Extended Kalman Filtering (EKF). However, there are issues due to the linearization approach in this algorithm, especially in case of strong model nonlinearities. This can lead to the EKF divergence, making the filter parameter tuning a difficult task. Moreover, linearization of the process dynamics can be complex to carry on and to implement. An alternative is to use the Unscented Kalman Filtering (UKF). This observer was first proposed in (Julier and Uhlmann, 1996). This filter uses a similar approach as the EKF, avoiding the linearization procedure. It leads to a better robustness and speed of convergence than the EKF (Kandepu *et al.,* 2008). This was also demonstrated for (bio)chemical processes (Romanenko *et al.,* 2004; Marafioti *et al.* 2008).

The aim of this paper is to design an UKF for biomass concentration estimation of a microalgae culture in a photobioreactor, based on available online measurements. More specifically, the paper deals with the estimation of microalga *C. reinhardtii* concentration in a torus photobioreactor, based on online measurements of CO_2 and O_2 molar fractions in the output gas. This paper is structured as follows: Material and methods used are presented in the first section. Then the process description together with its

Copyright © 2013 IFAC

modelling will be given in the second section. Third section describes the UKF algorithm and its application to the considered problem. The last section will present the results displayed, and finally some conclusions and perspectives are addressed.

2. MATERIALS AND METHODS

The studied microalga was a wild type *C. reinhardtii* strain 137AH from a culture collection of French Atomic Energy Center (Cadarache, France). The culture medium used for the photosynthetic growth of the green alga was an autotrophic minimum growth medium (MGM) which consisted in: $NaHCO_3$ – 1.68 g·L^{-1}, NH_4Cl – 1.45 g·L^{-1}, $MgSO_4{\cdot}7H_2O$ – 0.28 g·L^{-1}, $CaCl_2{\cdot}2H_2O$ – 0.05 g·L^{-1}, KH_2PO_4 – 0.61 g·L^{-1} and Hutner's trace elements – 1 mL·L^{-1}.

The photobioreactor used in the experiments is a lab-scale torus-shape one, illuminated on one side. It has a working volume of 1.47 L and a thickness of 4 cm. The incident light flux is provided by an electroluminescent diode panel calibrated with a LI-COR light meter LI-1400. It is further described in (Fouchard *et al*., 2008).

The pH was measured with a Mettler Toledo® Inpro 3253SG/120/Pt100 electrode connected to a Mettler Toledo® pH2050e. The temperature was measured by the same electrode and automatically compensates the pH.

The volumetric flows of the input gases (CO_2 and N_2) and of the output mixture of gases were measured by three Bronkhörst® HIGH TECH EL-FLOW type flow meters. The input flow meters are provided with proportional valves which allow the adjustment of the desired gas flow rate in percentage of the measuring range. The flow of fresh medium is regulated by a diaphragm pump Stepdos® FEM 1.08 on a range of 0.01 – 30 mL·min^{-1}.

3. PROCESS DESCRIPTION AND MODELING

The studied bioprocess consists in photoautotrophic growth of the green alga *C. reinhardtii* under light limiting conditions.

Microalgae are able to absorb CO_2 as major substrate and to generate O_2 as residue from the water oxidation reaction induced by the light as source of energy. Once the CO_2 dissolves in water, new ionic species are formed (*i.e.* dissolved carbon dioxide - $CO_{2,aq}$, bicarbonate - HCO_3^- and carbonate - CO_3^{2-}) through a series of reactions such as hydration, dehydration and protonation. When $CO_{2,aq}$ is removed from the medium as a result of the photosynthetic growth, the equilibrium of the bicarbonate buffer system ($CO_{2,aq} + H_2O \leftrightarrow H^+ + HCO_3^- \leftrightarrow 2H^+ + CO_3^{2-}$) will shift to the left and the pH will increase. The small volumes of CO_2 gas injected in the culture will shift back the equilibrium and the pH will decrease.

The dynamic model describes the behavior of microalgae cultures with a set of nonlinear algebro-differential equations deduced from mass balance considerations on both liquid and gaseous phases, assuming well mixed conditions. A radiative model, which expresses the light attenuation inside the culture was coupled with a kinetic model for describing the light-driven processes characterizing microalgae growth. It results in using a particular class of models returning local photosynthetic responses by expressing the specific growth rate as a function of local irradiance in the depth of the culture (z). The average photosynthetic response $\langle r_X \rangle$ calculated all over the reactor's volume was obtained by integrating the local photosynthetic responses on the direction of the culture depth.

The mechanistic dynamical model employed for describing all these phenomena was developed in (Ifrim, 2012).

The time evolution of the system can be described through five state variables: the biomass concentration (denoted X), the dissolved inorganic carbon (DIC) concentration (denoted C_{DIC}), the dissolved O_2 concentration (denoted C_{O_2}) and the CO_2 and O_2 molar fractions in the output gas (denoted resp. $y_{out}^{CO_2}$ and $y_{out}^{O_2}$). These last are defined by $y_{out}^{\varepsilon} = G_{out}^{\varepsilon} / G_{out}$, where G_{out} is the total output gas.

As long as the other nutrients are present in the culture medium in excess (nonlimiting concentrations), their evolution is not considered, since it is assumed that they have no influence on the growth.

3.1 Mass balance in liquid phase

The state variables describing the liquid phase have been expressed in terms of mass balance equations as follows (batch mode):

$$\frac{dX}{dt} = \langle r_X \rangle \tag{1}$$

$$\frac{dC_{DIC}}{dt} = -\frac{\langle r_X \rangle}{M_X} + N_{CO_2} \tag{2}$$

$$\frac{dC_{O_2}}{dt} = \frac{\langle r_X \rangle . Q_p}{M_X} + N_{O_2} \tag{3}$$

where $\langle r_X \rangle$ the average volumetric growth rate, M_X the C-mole mass and Q_p the photosynthetic quotient. N_{CO_2} (resp. N_{O_2}) is the volumetric mass transfer rate for CO_2 (resp. O_2). They can be expressed as follows:

$$N_\varepsilon = k_L a_\varepsilon . \left(\frac{P}{H_\varepsilon} y_{out}^{\varepsilon} - C_\varepsilon \right) \tag{4}$$

where subscript ε represents the component (CO_2 or O_2), $k_L a_\varepsilon$ the volumetric mass transfer coefficient, H_ε the Henry constant at 25°C and P the pressure.

Moreover, CO_2 concentration is not measured and it is calculated from the DIC concentration and pH as follows:

$$C_{CO_2} = C_{DIC} / (1 + K_1 10^{pH} + K_1 K_2 10^{2pH}) \tag{5}$$

where K_1, K_2 are the equilibriums constants (Edwards *et al.*, 1978).

3.2 Mass balance in gaseous phase

Based on the ideal gas law and gas balance, the molar fractions of output gases have been expressed as follows:

$$\frac{dy_{out}^{CO_2}}{dt} = \frac{RT}{PV_g} \left(y_{in}^{CO_2} G_{in} - y_{out}^{CO_2} . G_{out} - V_l . N_{CO_2} \right) \tag{6}$$

$$\frac{dy_{out}^{O_2}}{dt} = \frac{RT}{PV_g} \left(y_{in}^{O_2} . G_{in} - y_{out}^{O_2} . G_{out} - V_l . N_{O_2} \right) \tag{7}$$

where R is the universal gas constant, T the temperature, V_g

(resp. V_l) is the gas (resp. liquid) volume. Subscript *in* denotes the input gas. Input and output gas flow-rates are related by:

$$G_{out} = y_{in}^{N_2}.G_{in}/(1 - y_{out}^{CO_2} - y_{out}^{O_2}) \quad (8)$$

where G_{in} represents the total volumetric flow rate at the PBR inlet and $y_{in}^{N_2}$ represents the molar fraction of gazous N_2 (an inert vector gaz).

3.3 Growth rate model

The average volumetric growth rate is expressed using a Haldane model of the photon flux density into the culture medium as follows:

$$\langle r_X \rangle = \langle \mu_0 \frac{I}{K_I + I + \frac{I^2}{K_{II}}} \rangle . X \triangleq \frac{1}{L}\int_0^L \mu_0 \frac{I}{K_I + I + \frac{I^2}{K_{II}}} dz \, . X \quad (9)$$

where K_I is the half-saturation constant, K_{II} the inhibition constant and μ_0 is related to the maximum specific growth rate (Dochain, 2008). z is the considered culture depth, L the photobioreactor total depth and I the irradiance distribution inside the photobioreactor. For the torus one, the analytical solution was obtained as follows (Ifrim, 2012):

$$I(z) = 2q_0 \frac{(1+\alpha)e^{\delta(L-Z)} - (1-\alpha)e^{-\delta(L-Z)}}{(1+\alpha)^2 e^{\delta L} - (1-\alpha)^2 e^{-\delta L}} \quad (10)$$

where q_0 represents the hemispherical incident light flux, δ is the extinction coefficient and α the linear scattering modulus.

The system model is thus made of five differential equations (1-3, 6, 7). Model parameters were identified on experimental data issued from batch cultures (Ifrim, 2012) and are given in Table 1.

Table 1. Model parameters

Parameter	Value	Unit
μ_0	0.16	h^{-1}
K_I	120	µmol m^{-2} s^{-1}
K_{II}	2500	µmol m^{-2} s^{-1}
M_x	27.8	gC-mole
Q_p	1.1	-
$(K_L a)_{O_2}$	0.9	h^{-1}
$(K_L a)_{CO_2}$	$0.8(K_L a)_{O_2}$	h^{-1}
P	1.1013 10^5	Pa
T	298.15	K
R	8.3145	J mol^{-1} K^{-1}
V_l	1.47 10^{-3}	m^3
V_g	$0.12 * V_l$	m^3
L	0.04	m
K_1	$10^{-6.35}$	-
K_2	$10^{-10.3}$	-
H_{O_2}	8.384 10^4	Pa $m^3 mol^{-1}$
H_{CO_2}	2903.8	Pa $m^3 mol^{-1}$
α	0.996	-
δ	172.69	-

Only two states are measured online: molar fractions in the output gas of carbon dioxide and oxygen, in addition to physical variables (pH, temperature and input and output flow-rates).

4. STATE ESTIMATION

4.1 Observability analysis

First, the system observability was checked using observability forms introduced in (Gauthier and Kupka, 1994). The state vector is expressed in the form of two partitions, where the second one contains the measured variables. In the considered system, the two partitions are given by: $x_1 = (X, C_{DIC}, C_{O_2})$ and $x_2 = (y_{out}^{CO_2}, y_{out}^{O_2})$.

The observability of the system is then assessed if the following condition is fulfilled (Dewasme *et al.*, 2013):

$$rank \frac{\partial f_2}{\partial x_1} = m \quad (11)$$

where m is the number of measurements (m=2) and f_2 is the dynamics of x_2 (i.e $\dot{x}_2 = f_2(x_1, x_2)$).

This condition translates that a disturbance of the measured states can be propagated to the other states. It was tested in the case of the studied problem, and it was assessed that CO_2 and O_2 molar fractions in the output gas are sufficient to reconstruct the other state variables for the considered experimental conditions.

4.2 Unscented Kalman Filter Algorithm

Due to systems strong nonlinearities and uncertainties, the UKF is used. Unlike the EKF, where the state distribution is propagated analytically through the first-order linearization of the nonlinear system, UKF is derivative-free.

The state distribution is represented using a minimal set of carefully chosen sampling points, called *sigma points*. Each of these points is then propagated through the nonlinearities, the mean and the covariance being extracted from these transformed points.

Let us consider the discrete-time nonlinear model:

$$x_{k+1} = F(x_k, u_k) + v_k \quad (12)$$

$$y_k = H(x_k) + w_k$$

where x is the state vector (dim(x)=n), u the input, F and H are nonlinear functions and v_k and w_k are process and measurement noise, respectively. The algorithm is thus as follows:

Initialization (k=0):

$$\hat{x}_0 = E[x_0],\ P_0 = E[(x_0 - \hat{x}_0)(x_0 - \hat{x}_0)^T] \quad (13)$$

For $k = 1, \dots, \infty$:

Step 1: Selection of the sigma points:

$$(\mathcal{X}_{k-1})_0 = \hat{x}_{k-1} \quad (14a)$$

$$(\mathcal{X}_{k-1})_i = \hat{x}_{k-1} + \gamma.\left(\sqrt{P_{k-1}}\right)_i,\ i = 1, \dots, n, \quad (14b)$$

$$(\mathcal{X}_{k-1})_i = \hat{x}_{k-1} - \gamma.\left(\sqrt{P_{k-1}}\right)_{i-n},\ i = n+1, \dots, 2n \quad (14c)$$

where $\left(\sqrt{P_{k-1}}\right)_i$ is the i-th column of the square root of the covariance matrix of the previous time step (calculated by Cholesky factorization). The parameter γ can be interpreted as a scaling factor used to move the position of sigma points around the mean value. It is given by: $\gamma = \sqrt{n+\lambda}$, where $\lambda = a^2(n+k_0) - n$ and (a, k_0) are parameters to be chosen. Generally, a has small values ($10^{-4} \leq a \leq 1$). k_0 is chosen so that $k_0 \geq 0$, to guarantee the semi-positive definiteness of the covariance matrix (in general k_0 is set to zero).

Step 2: Prediction. The sigma points are propagated through the nonlinear dynamics and the estimation of the predicted state is calculated:

$$\mathcal{X}_{k|k-1} = F[\mathcal{X}_{k-1}, u_{k-1}] \quad (15)$$

$$\hat{x}_k^- = \sum_{i=0}^{2n} W_i^{(m)} \mathcal{X}_{i,k|k-1} \quad (16)$$

The predicted covariance is then computed:

$$P_k^- = \sum_{i=0}^{2n} W_i^{(c)} \left[\mathcal{X}_{i,k|k-1} - \hat{x}_k^-\right]\left[\mathcal{X}_{i,k|k-1} - \hat{x}_k^-\right]^T + Q \quad (17)$$

where Q is the process noise covariance matrix.

Step 3: Update. By using the predicted sigma points (15) and covariance (17), a new set of sigma points is calculated which are projected through the observation model. The predicted measurements are then given by:

$$\mathcal{Y}_{k|k-1} = H\left[\mathcal{X}_{k|k-1}\right] \quad (18)$$

$$\hat{y}_k^- = \sum_{i=0}^{2n} W_i^{(m)} \mathcal{Y}_{i,k|k-1} \quad (19)$$

The covariance of the innovation and the cross-covariance matrix are then given by:

$$P_{\tilde{y}_k\tilde{y}_k} = \sum_{i=0}^{2n} W_i^{(c)} \left[\mathcal{Y}_{i,k|k-1} - \hat{y}_k^-\right]\left[\mathcal{Y}_{i,k|k-1} - \hat{y}_k^-\right]^T + R_n \quad (20)$$

$$P_{y_k x_k} = \sum_{i=0}^{2n} W_i^{(c)} \left[\mathcal{X}_{i,k|k-1} - \hat{x}_k^-\right]\left[\mathcal{X}_{i,k|k-1} - \hat{x}_k^-\right]^T \quad (21)$$

where R_n is the measurement noise covariance.

The estimations are updated by using the classical Kalman filter equations:

$$\mathcal{K}_k = P_{y_k x_k} P_{\tilde{y}_k\tilde{y}_k}^{-1} \quad (22)$$

$$\hat{x}_k = \hat{x}_k^- + \mathcal{K}_k(y_k - \hat{y}_k^-) \quad (23)$$

$$P_k = P_k^- - \mathcal{K}_k P_{\tilde{y}_k\tilde{y}_k} \mathcal{K}_k^T \quad (24)$$

Step 4: Repeat Steps 1 to 3 for the next sample.

The weighting factors used above are calculated as in:

$$W_0^{(m)} = \frac{\lambda}{n+\lambda}, W_0^{(c)} = \frac{\lambda}{n+\lambda} + 1 - \alpha^2 + \beta$$
$$W_i^{(m)} = W_i^{(c)} = \frac{1}{2(n+\lambda)} \quad (25)$$

where β is used to incorporate prior knowledge of the distribution of the state. It is a tuning parameter.

It can be noticed that in the UKF algorithm, Jacobian matrices are not needed as in the EKF one, leading to an easier implementation.

4.3 UKF parameters tuning

As for the EKF, the UKF has two initialization tuning parameters: the process and measurement noise covariance matrices (resp. Q and R_n). The second one depends on the sensor characteristics and is fixed by errors statistics of the measurement devices. The process covariance matrix Q is generally unknown and is thus tuned, by a trial-and-error method, so that the filter gives good estimation behaviour (accuracy, speed and good convergence).

Choosing the covariance matrix Q is generally a difficult task, especially in the case of nonlinear uncertain systems, since they do not satisfy the assumptions of normal distribution. Several approaches were proposed in literature to compute this matrix (by adaptive filtering or by optimization approach). In this paper, this matrix was determined by taking into account parameter uncertainty in the model, by linearization of the nonlinear system dynamics around the nominal parameter values (Valappil and Georgakis, 2000).

Let us consider the dynamic system:

$$\dot{x} = f(x, u, \theta) + v \quad (26)$$

$$y = H(x, \theta) + w$$

where θ are the model parameters.

Covariance of process noise v can be approached by linearizing the process dynamics around nominal trajectory and nominal parameters values (Valappil and Georgakis, 2000), leading to:

$$Q = \left(\frac{\partial f}{\partial \theta}\right)_{\theta_{nom}} . Q_0 . \left(\frac{\partial f}{\partial \theta}\right)_{\theta_{nom}}^T \quad (27)$$

where Q_0 is the parameter covariance matrix. It can be computed along with the identification procedure. In this paper, the parameter vector is chosen as:

$$\theta = \left(\mu_0, M_x, Q_p, (K_L a)_{O_2}\right) \quad (28)$$

Indeed, a sensitivity analysis shows that the considered model quality strongly depends on these parameters accuracy. In addition, these parameters are found to be the most uncertain when determined in the identification procedure.

5. RESULTS AND DISCUSSION

The UKF algorithm was implemented and tested on experimental data collected from various cultures of the considered microalga, in batch mode. In the sequel, two data sets are used, corresponding to two cultures, over 200h, with different incident light flux: in the first case (culture 1), q_0=300 µmol m^{-2} s^{-1} and in the second one (culture 2), q_0=110 µmol m^{-2} s^{-1}. Initial conditions of the cultures are similar and are given in Table 2.

Online measurements are collected with a sampling time equal to 5 min.

Since, the dynamical model (1-3, 6, 7) is continuous, it is discretized using an Euler scheme. The UKF parameters are chosen as follows: a=10^{-4}, $k_0 = 0$ and β=2 (optimal choice for a Gaussian distribution). Measurement and process noise covariance matrices are the same in the two cases and are chosen constant. Process covariance matrix is computed with (27), considering state values at the initial time.

Figures 1 to 3 illustrate results obtained in the case of the first culture, and figures 4 to 6 for the second one.

For the first experiment, the estimator has a better performance than the identified model in estimating biomass concentration (Fig. 1). Indeed, estimated values are close to off-line *X* measurements, whereas model over-estimate biomass concentrations. For the *DIC* and dissolved oxygen concentrations (Fig. 2 and 3), model predicted and estimated values are similar. However, estimated values are more fluctuating, because of periodic injection of carbon dioxide for pH regulation. No off-line measurements were available to assess the estimation accuracy.

Table 2. Initial state values

Parameter	Value	Unit
X(0)	0.2	g L^{-1}
$c_{TIC}(0)$	0.02	mol L^{-1}
$c_{O_2}(0)$	0	mol L^{-1}
$y_{out}^{CO_2}(0)$	0.005	-
$y_{out}^{O_2}(0)$	0.005	-

The second experiment enhances the estimator efficiency to reconstruct biomass concentrations (Fig. 4). From Fig. 5, it can be noticed that both of predicted and estimated DIC concentrations are lower than the off-line measurements (which are measured for this culture). However, estimator seems to converge to real values after 150h. In order to improve the estimator behaviour, one solution could be to identify, online, the parameters of the DIC concentration dynamics. Figure 6 shows that predicted and estimated dissolved oxygen concentrations are close, similarly to the results in the case of the first experiment.

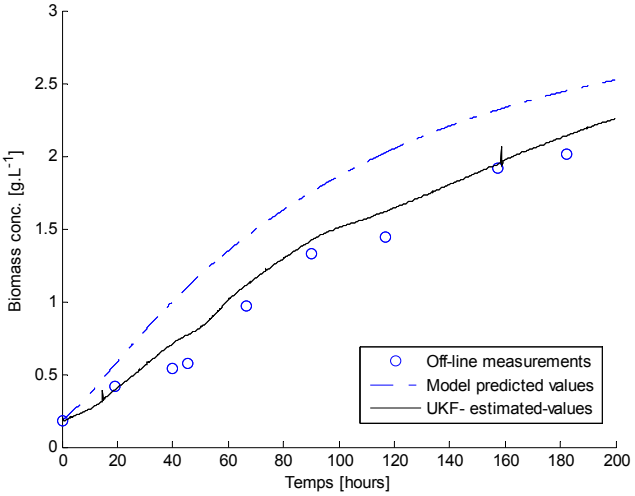

Fig.1. Time evolution of biomass concentration for culture 1 (q_0=300 µmol m^{-2} s^{-1})

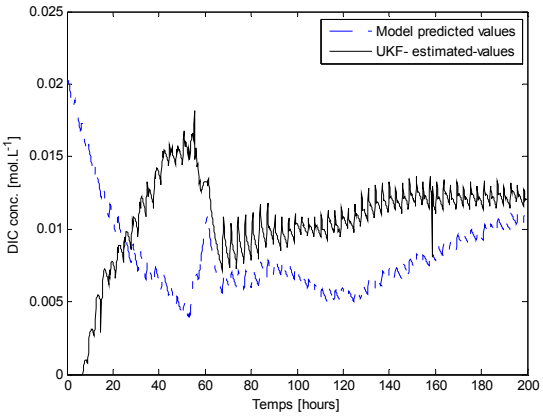

Fig. 2. Time evolution of DIC concentration for culture 1 (q_0=300 µmol m^{-2} s^{-1})

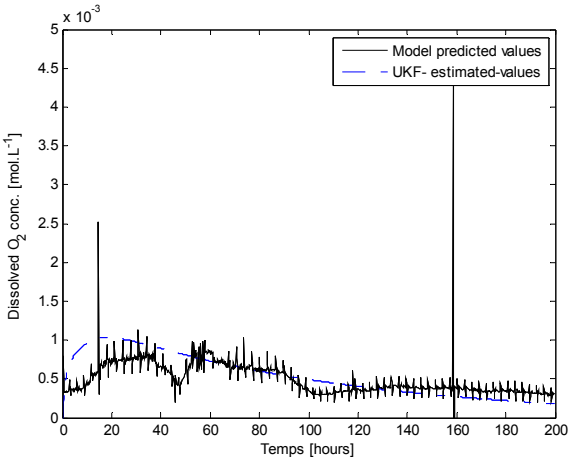

Fig. 3. Time evolution of dissolved O_2 concentration for culture 1 (q_0=300 µmol m^{-2} s^{-1}),

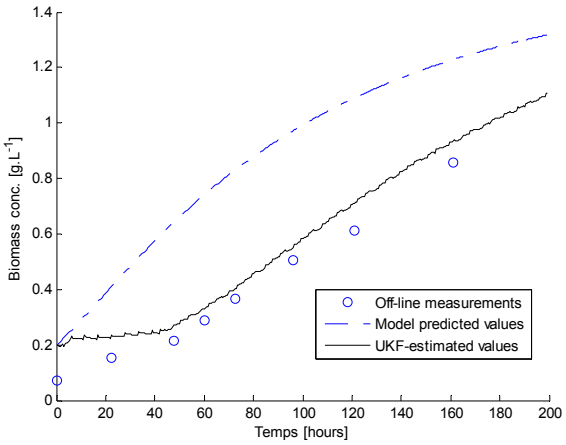

Fig.4. Time evolution of Biomass concentration for culture 2 (q_0=110 µmol m^{-2} s^{-1})

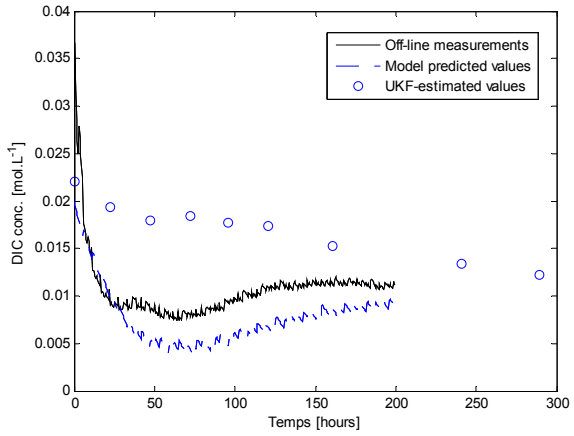

Fig. 5. Time evolution of DIC concentration for culture 2 (q_0=110 µmol m^{-2} s^{-1})

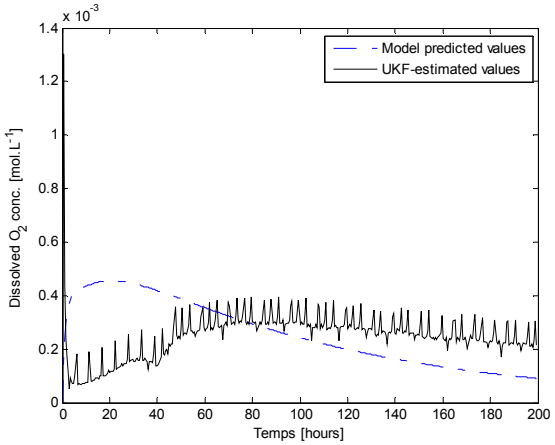

Fig. 6. Time evolution of dissolved O_2 concentration for culture 2 (q_0=110 µmol m^{-2} s^{-1})

6. CONCLUSIONS

The UKF estimation approach gives an accurate online estimation of the biomass concentration in a photobioreactor. UKF is easier to implement than an EKF algorithm, since it is derivative-free. Thus, the system model could be easily modified, for example to introduce substrate limitation or inhibition in the growth model.

Ongoing work considers the comparison of the proposed estimation strategy to the EKF one, showing that the UKF gives either similar or better results than the EKF. This comparison study will be continued in order to evaluate the UKF efficiency, convergence and robustness. The validation of the proposed estimation strategy on other experimental data, especially in the case of continuous cultures, will be also studied.

ACKNOWLDGMENTS

Authors wish to acknowledge support from the Romanian-French research cooperation project PACBIO.

REFERENCES

Bastin G, Dochain D. (1990) Online estimation and adaptive control of bioreactor, Process Measurement and Control, Vol. 1. Elsevier, Amsterdam

Su WW, Li J, Xu NS (2003) State and parameter estimation of microalgal photobioreactor cultures based on local irradiance measurement. *J Biotechnol* 105:165–178

Rapaport A, Dochain D (2005) Interval observers for biochemical processes with uncertain kinetics and inputs. *Math Biosci* 193(2):235–253

Goffaux G, Vande Wouwer A, Bernard O (2009) Improving continuous discrete interval observers with application to microalgae-based bioprocesses. *J Process Control* 19(7):1182–1190

Julier, S.J., Uhlmann, J.K. (1997) A new extension of the Kalman filter to nonlinear systems, In Proceedings of *Int. Symp. Aerospace/Defense sensing, Simul. And Controls*, 182-193.

Kandepu, R. Foss, B., Imsland, L. (2008) Applying the unscented Kalman filter for nonlinear state estimation, *J. Process Contr.*, 18, 753-768.

Romanenko, A., Castro, J. (2004) The unscented filter as an alternative to the EKF for nonlinear state estimation: a simulation case study, *Computers and Chemical Engineering*, 28(3), 347-355.

Marafioti, G., Tebbani, S., Beauvois, D., Becerra-Celis, G., Isambert, I., Hovd, M. (2009) Unscented Kalman filter and parameter estimation in a photobioreactor for microalgae production, In proceedings of *Int. Symp. on Adv. Contr. of Chem. Proc.*, Istanbul, Turkey.

Fouchard, S., J. Pruvost, B. Degrenne, J. Legrand, (2008) Investigation of H2 production using the green microalga Chlamydomonas reinhardtii in a fully controlled photobioreactor fitted with online gas analysis, *Int. J. Hydrogen Energy*. 33, 3302-3310.

Ifrim, G.A (2012) Control of Two Biological Processes of Environmental Interest (biological wastewater treatment and microalgae production in photobioreactor), PhD thesis, University of Nantes, France or University "Dunărea de Jos", Galaţi, Romania.

Edwards TJ, Maurer G, Newman J, Prausnitz JM. (1978) Vapour-liquid equilibria in multicomponent aqueous solutions of volatile weak electrolytes. *AIChE Journal*.24:966-975.

Dochain, D., (2003) State and parameter estimation in chemical and biochemical processes, *J. Process Contr.*, 13(8).

Gauthier, J.-P., Kupka I. (1994) Observability and observers for nonlinear systems, SIAM Journal Control and Optimization, 32(4), 975-994.

Dewasme, L., Goffaux, G., Hantson, A.-L., Vande Wouwer A. (2013) Experimental validation of an Extended Kalman Filter estimating acetate concentration in *E. coli* cultures, *Journal of Process Control*, 23, 148-157.

Valappil, J., Georgakis C. (2000) Systematic of state noise statistics for extended Kalman filters. *AIChE*, 46(2), 292-398.